

## Formation of nickel nanodots on GaN

D. Aurongzeb, K. Bhargava Ram, and M. Holtz<sup>a)</sup>  
*Department of Physics, Texas Tech University, Lubbock, Texas 79409*

M. Basavaraj, G. Kipshidze, B. Yavich, S. A. Nikishin, and H. Temkin  
*Department of Electrical Engineering, Texas Tech University, Lubbock, Texas 79409*

(Received 11 July 2005; accepted 22 November 2005; published online 11 January 2006)

We examine the annealing-induced formation of nickel nanodots on GaN substrates. The initial Ni layer thickness is 2 nm. Annealing temperatures range from 550 to 930 °C. The islands are well defined at the highest temperatures. Island formation kinetics provide an activation energy of  $0.34 \pm 0.07$  eV. Time dependence of the nanodot island areas, annealed at 750 °C, is consistent with a  $t^{2/3}$ . These observations are indicative of diffusion-limited ripening as the primary formation mechanism. X-ray diffraction results show that nickel gallides form at anneal temperatures 750 °C and above. © 2006 American Institute of Physics. [DOI: 10.1063/1.2159077]

### I. INTRODUCTION

Self-assembly has drawn considerable attention for producing nanometer-scale structures<sup>1–3</sup> for applications in electronic, optoelectronic, and magnetic devices. Formation of self-assembled structures generally depends on competition between the surface and interfacial free energies, and is most significant in ultrathin layers. The physics of island formation has been studied<sup>4,5</sup> with the most attention devoted to semiconductor nanodots forming on semiconductors. Few experiments concern metallic nanostructures on semiconductor surfaces. The problem of metal self-assembly on semiconductors is important, for example, in contact metallization<sup>6</sup> and in the vapor-liquid-solid growth mechanism for semiconducting nanowires.<sup>7,8</sup> Upon high-temperature processing, there is also the possibility of the metal and semiconductor chemically interacting at the interface to produce unwanted compounds.<sup>9</sup>

In this paper, we report studies of nickel nanodot formation when ultrathin (2 nm) layers are deposited on epitaxial GaN. This is a physically interesting combination because the surface energies of Ni and GaN are closely matched,<sup>10,11</sup> so that island nucleation is only slightly favored. We observe Ni nanodots to form following annealing at temperatures 550 °C and above. We examine the kinetics of nanodot formation and the time dependence through surface analysis using atomic force microscopy (AFM) and magnetic force microscopy (MFM). In addition to the physically interesting Ni nanodots formation on GaN, the situation is somewhat complicated by the known reaction between Ni and GaN to form nickel gallides.<sup>6</sup> We study this formation using x-ray diffraction (XRD). The nanodot formation is found to be consistent with surface-diffusion-based ripening.

### II. EXPERIMENTAL METHODS

The starting GaN layers were grown epitaxially on sapphire substrates by TDI, Inc. A nickel layer with 2 nm thickness was deposited using e-beam evaporation at the rate of

$\sim 1$  Å/s in a vacuum chamber with base pressure  $\sim 10^{-7}$  Torr. Annealing was carried out in N<sub>2</sub> atmosphere ( $\sim 550$  Torr) to reduce the possible effects of oxidation. The temperature of the anneal chamber was varied from 550 to 930 °C to include the range at which decomposition of the GaN initiates (700–800 °C)<sup>12</sup> and at which reactions occur forming nickel gallides ( $>600$  °C).<sup>6</sup> We also studied the time dependence of the surface properties for anneals up to 40 min long at 750 °C. Nanodot formation slows after  $\sim 30$  min of annealing at this temperature. For the temperature dependence we thus use 30 min anneals. Pre- and post-annealing surfaces were analyzed using combined AFM and MFM. *Ex situ* AFM provides surface topography of the Ni nanodots, while the MFM allows us to examine Ni coverage and nanodot formation. Root-mean-square (RMS) roughness ( $\sigma_{\text{RMS}}$ ) was analyzed for the AFM measurements according to

$$\sigma_{\text{RMS}}^2 = \frac{1}{A} \iint_A [z(\mathbf{r}) - \bar{z}]^2 d\mathbf{r} \rightarrow \frac{1}{(N-1)(M-1)} \sum_{i,j}^{N,M} (z_{i,j} - \bar{z})^2, \quad (1)$$

where  $z$  is the height at  $\mathbf{r}=(x,y)$  coordinate, denoted  $(i,j)$  in discretized form, and  $\bar{z}$  is the mean height. For images analyzed here,  $N=M=512$  in the images spanning area  $A=1 \mu\text{m} \times 1 \mu\text{m}$ . Scanning electron microscopy was also used to examine the nanodots, although we do not focus on those images in this paper.

The as-deposited layers are seen to fully cover the GaN surface and are smooth with  $\sigma_{\text{RMS}}=0.6 \pm 0.2$  nm. This value is comparable to the substrate roughness, which also exhibits the characteristic steplike surfaces typical of two-dimensional growth mode. In Fig. 1 we show combined (i.e., simultaneous) AFM and MFM scans of the Ni surfaces following two different anneals. Images (a) and (b) are AFM and MFM, respectively, after annealing at 930 °C for 30 min. Clearly seen are nanodot formations with lateral size ranging from 150 to 250 nm and regular shapes. The best formed nanodots are hexagonal in shape. The MFM confirms full

<sup>a)</sup>Electronic mail: Mark.Holtz@ttu.edu

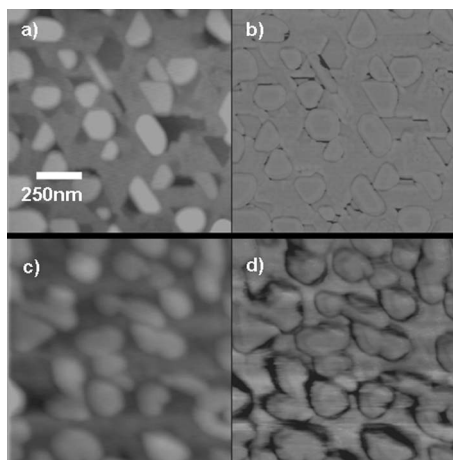


FIG. 1.  $1\ \mu\text{m} \times 1\ \mu\text{m}$  images of Ni surfaces on GaN substrates following two different anneals: (a) and (b) combined AFM and MFM, respectively, following  $930\ \text{°C}$  for 30 min; (c) and (d) combined AFM and MFM, respectively, following  $750\ \text{°C}$  for 20 min. Full gray scale ranges are (a) 15.0 nm and (c) 17.8 nm.

coverage by Ni, i.e., the areas surrounding the Ni islands have not fully depleted the available Ni. Images (c) and (d) are AFM and MFM, respectively, after annealing at  $750\ \text{°C}$  for 20 min. At this temperature, the nanodot shapes are not as well defined as at the higher temperature. Note that we annealed at  $750\ \text{°C}$  for up to 40 min, and the observed shapes never appear as distinct as what we show in Fig. 1(a) and 1(b). Figure 1(d) also confirms coverage by the Ni and magnetization of the Ni nanodots.

### III. FORMATION KINETICS

We observe the nanodot height to increase from  $\sim 1\ \text{nm}$  following  $550\ \text{°C}$  anneal (30 min) to  $\sim 5\ \text{nm}$  after annealing at  $750\ \text{°C}$ . In Fig. 2 we summarize the temperature dependence of Ni nanodot growth following anneals of 30 min duration in an Arrhenius plot. The lateral size of the nanodots is determined using a histogram of the island dimension, directly from the AFM and MFM images. The dependence is fit equally well by Gaussian or log-normal dependences; we use the former. The error bars shown are the standard deviations of the Gaussian fits. The lateral size is seen to increase

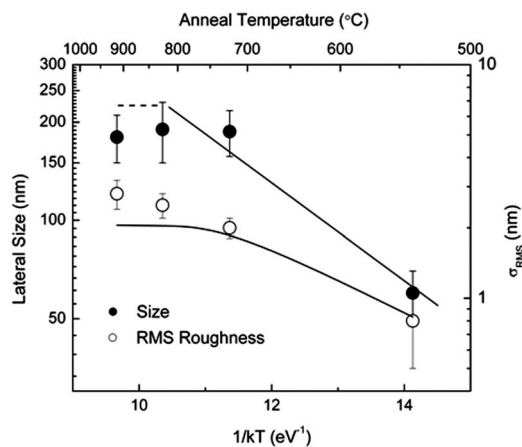


FIG. 2. Arrhenius plot of nanodot lateral size and RMS surface roughness.

with anneal temperature. At each temperature, we also examined the island height to lateral size ratio versus island volume. This ratio is found to be constant, indicating that the island shapes obtained are stable to internal body and substrate stresses.<sup>13</sup>

The data trend in Fig. 2 for lateral size is consistent with activated behavior with activation energy  $E_A = 0.34 \pm 0.07\ \text{eV}$ . Our previous work of Ni nanodot formation on silicon substrates provided two activation energies.<sup>2</sup> For temperatures below  $500\ \text{°C}$  we obtained  $E_A$  of  $0.09 \pm 0.02\ \text{eV}$ , while above  $600\ \text{°C}$  we found  $E_A$  of  $0.31 \pm 0.05\ \text{eV}$ . Calculated values of Ni self-diffusion across major crystal facets are  $E_A(111) = 0.063\ \text{eV}$ ,  $E_A(110) = 0.39\ \text{eV}$ , and  $E_A(100) = 0.68\ \text{eV}$ .<sup>14</sup> We thus interpreted our results to indicate surface self-diffusion across (111) facets as the primary formation mechanism in the low-temperature range, and the high-temperature formation to stem from surface self-diffusion across (110) facets oriented parallel to the substrate surface. Our current measured  $E_A$  result was obtained across the range  $550\text{--}930\ \text{°C}$  and thus corresponds to the high-temperature range studied in Ref. 2. The  $E_A = 0.34 \pm 0.07\ \text{eV}$  value is within the experimental error of our corresponding activated surface diffusion of Ni on (110) surfaces. We note that the rate of ascent in nanocrystal size with anneal temperature slows at the high end. This may be due to the strong interaction between Ni and GaN as the latter decomposes, and due to depletion of the Ni reservoir as nickel gallides form (discussed later). By including the highest temperature point in Fig. 2 we obtain  $E_A = 0.27 \pm 0.07\ \text{eV}$ , which is also within error of our prior result and does not change our discussion. The formation kinetics are thus consistent with diffusion-driven growth primarily across the (110) crystal surface.

The well-formed Ni nanodots have flat, horizontally oriented top surfaces and sidewalls, which make angles ranging from  $14^\circ$  to  $18^\circ$  from the horizontal. These angles do not lend themselves to straightforward Wulff construction, as was used in Ref. 2. The deficiency of low-order crystal facets in the nanocrystals formed here is consistent with the lack of surface diffusion pinning and the absence of self-limited growth. There are several reasons for the Ni on GaN behavior to differ from Ni on Si. First, surface energy densities are  $2.011\text{--}2.426\ \text{J/m}^2$  for Ni<sup>10</sup> and  $1.6\ \text{J/m}^2$  for GaN.<sup>11</sup> The small surface energy density mismatch between Ni and GaN suggests a weak island nucleation, i.e., the formation of larger clusters. In our experiments, we observe a tendency for Ni to form islands, but the MFM results show Ni to remain across the entire surface. In contrast, the surface energy density for silicon is smaller,<sup>10</sup> producing a strong tendency to form islands with higher sidewall slopes. Second, Ni reacts with GaN at the temperatures studied here. The formation of Ni-Ga intermetallic compounds at the interface is expected to change the interaction energies, and thus the wetting versus island nucleation properties. As a result of these effects, the Ni formations on GaN have different faceting properties. These play a strong role in nanodot formation and produce ripening, which we return to later.

The RMS roughness is also shown in Fig. 2. The trend seen of increasing roughness with anneal temperature is il-

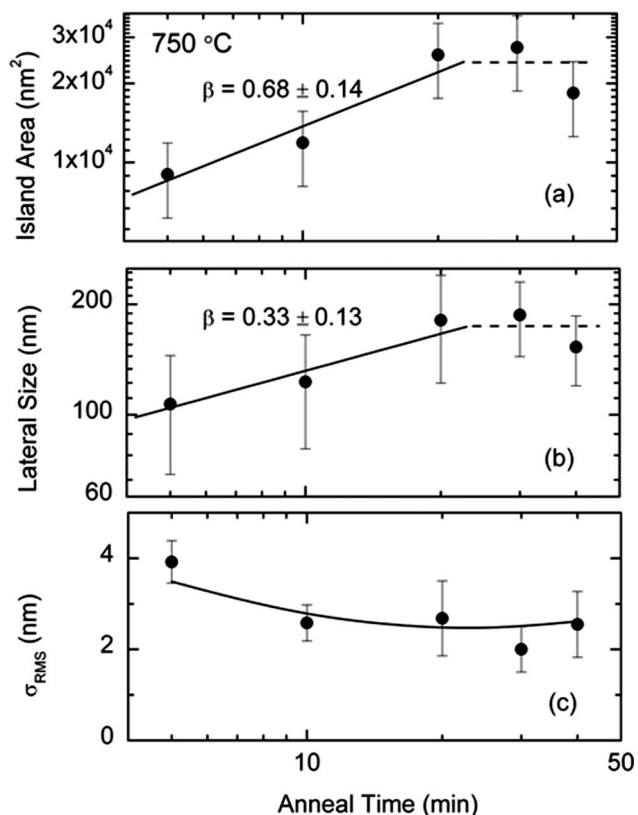


FIG. 3. Time dependence of (a) nanodot area (log-log), (b) lateral nanodot size (log-log), and (c) RMS roughness (lin-log).

illustrative of island formation. Following Ref. 2, we link the  $\sigma_{\text{RMS}}$  dependence with nanodot formation using the definition in Eq. (1) and the dimensionless area fill factor defined as  $f_A = nA_0$ , where  $n$  is the number of islands per unit area and  $A_0$  is the average island area. By straightforward integration we obtain

$$\sigma_{\text{RMS}} = \sqrt{nA_0(1 - nA_0)}h, \quad (2)$$

where  $h$  is the average height of the islands. This analysis is appropriate when the island height distribution is narrow. Using density dependence and  $h$  from analysis of the AFM images, we arrive at the lower curve shown in Fig. 2. The good agreement between the measured  $\sigma_{\text{RMS}}$  and this straightforward analysis supports, on statistical grounds, the uniformity in our nanodot formation.

#### IV. FORMATION DYNAMICS AT 750 °C

We examine the nanodot formation of Ni annealed at 750 °C and for times ranging from 5 to 40 min. Results are summarized in Fig. 3. In the log-log graph in Fig. 3(a), we see the average island area  $A$  increase with time. Growth mode can be examined through the area scaling  $A \propto t^\beta$ . Two dependences are typical for island growth.<sup>15</sup> When  $A$  depends on time like  $t^{2/3}$ , then the formation process is diffusion-limited ripening. When  $A$  is directly proportional to anneal time, the formation process is said to be diffusion attachment-reattachment limited. From our results we find a time exponent of  $\beta = 0.68 \pm 0.13$ , up to 30 min, after which the island growth saturates. We attribute the saturation to

depletion of the Ni reservoir remaining on the surface. This is consistent with diffusion-limited nanodot formation, and suggests a ripening process. The island size distribution at each anneal is also indicative of ripening. It is also consistent with the island shapes discussed above, with shallow side-wall angles that should not favor attachment-reattachment to specific sites (pinning). In Fig. 3(b) we also graph the dependence of lateral island size on anneal time. The scaling exponent here is 1/2 of what we obtain for the island area, which is obviously expected.

Figure 3(c) shows the RMS roughness dependence (semilog) on anneal time. The as-deposited samples have smooth surfaces, with  $\sigma_{\text{RMS}} = 0.6 \pm 0.2$  nm. A brief anneal of 5 min raises the roughness considerably as the island formation process begins. The nanodots seen after this anneal are relatively poorly formed, although they have a uniform size distribution. For longer anneal periods, the island surfaces become flatter, and the sizes and shapes are not regular due to ripening and because the temperature of this anneal is too low to produce well-shaped structures. By 850 °C we see the onset of well-defined structures, similar to Fig. 1(a). Also shown in Fig. 3(c) is the calculated dependence of Eq. (2) obtained as described above. The good agreement between the calculation and the data is consistent with uniform island heights following each anneal.

#### V. FORMATION OF NICKEL GALLIDES

As mentioned, the GaN decomposition and nickel-gallide formation temperatures are in the range of anneal conditions we examine here. In order to examine if any chemical interaction has taken place, we carried out XRD measurements pre- and post-annealing. Figure 4(a) shows an XRD pattern following anneal at 930 °C for 30 min. The dominant features are from the GaN layer, along with several diffraction bands stemming from the sapphire. The strong features are from diffraction of the Cu  $K\beta$  radiation and the replica peaks are from the Cu  $K\alpha$ . After annealing we observe the presence of a strong diffraction band at  $\sim 43.7^\circ$ , as shown in Fig. 4(b). These appear following annealing at 750 °C and above, and are attributed to nickel-gallide phase Ni<sub>3</sub>Ga<sub>4</sub>,<sup>16</sup> which may precipitate from the solid solution of Ni and Ga at the interface.<sup>17</sup> Additionally, we observe diffraction at  $\sim 53.3^\circ$ , which is consistent with the presence of Ga. These results confirm previous reports that GaN decomposes<sup>12</sup> and that nickel gallides form in this temperature range.<sup>6</sup> Arrhenius analysis of the Ni<sub>3</sub>Ga<sub>4</sub> diffraction intensity gives us an activation energy  $E_A = 0.6 \pm 0.1$  eV. This low  $E_A$  may be primarily associated with interdiffusion and formation of this compound. In addition, this peak is found at higher diffraction angle than the reference material, and to systematically shift toward the reference value of  $43.384^\circ$  with higher anneal temperature. This may be due to the presence of stress in the early formation stages and a slight relaxation with higher temperature.

In addition, we also observe in Fig 4(a) weaker features at  $\sim 53^\circ$  and  $96^\circ$ , which we attribute to the presence of NiGa<sub>4</sub>. By tracking the intensity versus anneal temperature, we obtain activation energy  $E_A = 2.5 \pm 0.2$  eV. This is consis-



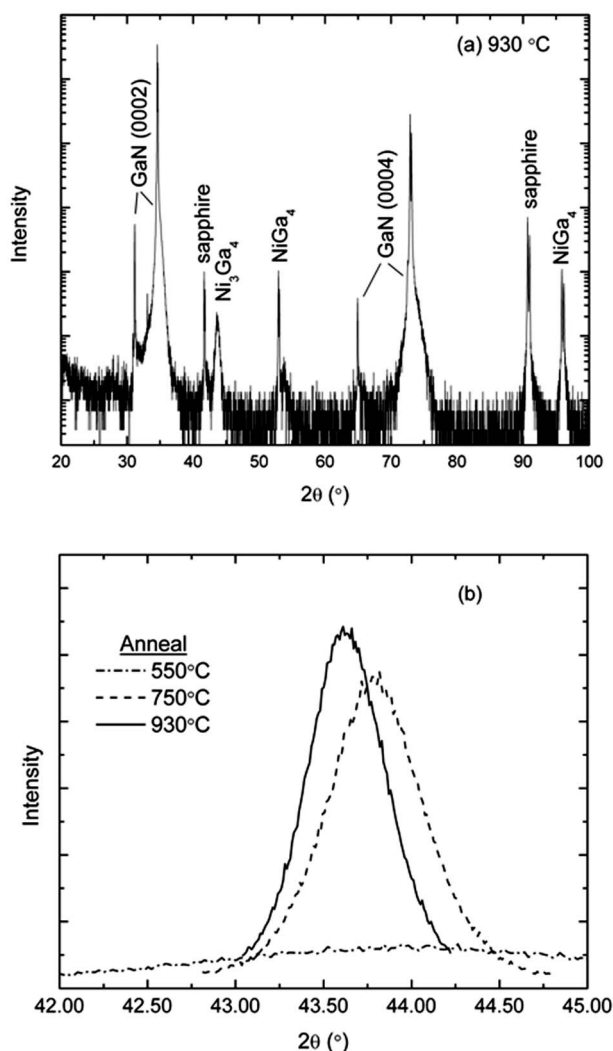


FIG. 4. XRD of the Ni-coated GaN following 30 min. (a) Full  $2\theta$  scan, note semilog scale. (b) Details of the  $\text{Ni}_3\text{Ga}_4$ -related diffraction peak following several anneals, linear intensity scale. No feature is observed in the as-deposited case.

tent with the expectation that more gallium-rich compounds will form at higher temperatures due to accelerated GaN decomposition.<sup>6</sup>

## VI. SUMMARY

We have observed Ni, deposited on GaN substrates with initial thickness 2 nm, to self-assemble into nanodots upon annealing. Poorly defined shapes are produced after low-temperature annealing (550 °C). The islands become more regular, reminiscent of hexagonal shapes, at higher temperature. By examining the kinetics, a nanodot activation energy of  $E_A = 0.34 \pm 0.07$  eV is obtained. This is consistent with surface diffusion as the primary formation mechanism. The time dependence, at anneal temperature 750 °C, is consistent with an island area proportional to  $t^{2/3}$ . This further confirms surface diffusion as the formation mechanism. In contrast to our

previous work on Ni nanodots formed on Si, the current situation is not self-limiting. This is attributed to differences in the wetting/nucleation behaviors of Ni on these two substrates and perhaps to the chemical reaction of Ni with GaN at high temperature. We do not observe distinct sidewall facets terminating the islands, and therefore do not expect diffusional pinning. We also note, based on MFM studies, that Ni fully covers the regions surrounding the nanodots. Both the temperature and time dependences observed here are indicative of ripening. The island size statistics are also in agreement with ripening, although it slows after long anneal times, possibly due to depletion of the available Ni.

One final note is that we observe what appears to be island drift in some of the AFM images after the highest anneal temperatures. This has been recently reported for SiGe islands on Si wafers when annealed at high temperatures.<sup>5</sup> The motion is related to redistribution of the substrate (Si) atoms through asymmetric diffusion in the nanodots (SiGe). In our case, it is the Ga atoms that may exhibit a similar interaction, and motion would be related to the formation of nickel gallides. XRD studies confirm that the latter compounds are formed in our experiments, and thus a similar “macroscopic” motion of the Ni nanodots is plausible in our experiments. Further work is needed to study this phenomenon in detail.

## ACKNOWLEDGMENTS

This study was supported in part by the National Science Foundation (Grants No. ECS-0 323 640, No. ECS-0 304 224, and No. CTS-0 210 141) and the J. F. Maddox Foundation.

- <sup>1</sup>H. Omi and T. Ogino, *Appl. Phys. Lett.* **71**, 2163 (1997).
- <sup>2</sup>D. Aurongzeb, S. Pantibandla, M. Holtz, and H. Temkin, *Appl. Phys. Lett.* **86**, 103 107 (2005).
- <sup>3</sup>J. Nogami, B. Z. Liu, M. V. Katkov, C. Ohbuchi, and N. O. Birge, *Phys. Rev. B* **63**, 233 305 (2001).
- <sup>4</sup>F. M. Ross, J. Tersoff, and R. M. Tromp, *Phys. Rev. Lett.* **80**, 984 (1998).
- <sup>5</sup>U. Denker, A. Rastelli, M. Stoffel, J. Tersoff, G. Katsaros, G. Costantini, K. Kern, N. Y. Jin-Phillipp, D. E. Jesson, and O. G. Schmidt, *Phys. Rev. Lett.* **94**, 216103 (2005).
- <sup>6</sup>H. S. Venugopalan, S. E. Mohney, B. P. Luther, S. D. Wolter, and J. M. Redwing, *J. Appl. Phys.* **82**, 650 (1997).
- <sup>7</sup>X. F. Duan and C. M. Lieber, *J. Am. Ceram. Soc.* **122**, 188 (2000).
- <sup>8</sup>G. Kipshidze, B. Yavich, A. Chandolu, J. Yun, V. Kuryatkov, I. Ahmad, D. Aurongzeb, M. Holtz, and H. Temkin, *Appl. Phys. Lett.* **86**, 033104 (2005).
- <sup>9</sup>H. S. Venugopalan, S. E. Mohney, J. M. DeLucca, B. P. Luther, and G. E. Bulman, *J. Vac. Sci. Technol. A* **16**, 607 (1998).
- <sup>10</sup>H. Zhou, D. Kumar, A. Kvit, A. Tiwari, and J. Narayan, *J. Appl. Phys.* **94**, 4841 (2003).
- <sup>11</sup>J. E. Northrup, J. Neugebauer, R. M. Feenstra, and A. R. Smith, *Phys. Rev. B* **61**, 9932 (2000).
- <sup>12</sup>O. Brandt, H. Yang, and K. H. Ploog, *Phys. Rev. B* **54**, 4432 (1996).
- <sup>13</sup>F. Silly and M. R. Castell, *Phys. Rev. Lett.* **94**, 046103 (2005).
- <sup>14</sup>U. Kürpick, *Phys. Rev. B* **64**, 075 418 (2001).
- <sup>15</sup>L. Fitting, M. C. Zeman, W.-C. Yang, and R. J. Nemanich, *J. Appl. Phys.* **93**, 4180 (2003).
- <sup>16</sup>*JCPDS-International Centre for Diffraction Studies* (1997), p. 130.
- <sup>17</sup>J. Groebner, R. Wenzel, G. G. Fisher, and R. Schmid-Fetzer, *J. Phase Equilib.* **20**, 615 (1999).